ORIGINAL ARTICLE

The effect of external flow on 3D orientation of a microscopic sessile suspension feeder, *Vorticella convallaria*

Tia Böttger[1,#] | Brett Klaassen van Oorschot[1,2,#] | Rachel E. Pepper[1]

[1]Department of Physics, University of Puget Sound, Tacoma, Washington, USA

[2]Biomimetics Lab, Experimental Zoology Group, Wageningen University, Wageningen, The Netherlands

Correspondences
Brett Klaassen van Oorschot, Experimental Zoology Group, Wageningen University, Wageningen, Gelderland 6708 PB, The Netherlands. Email: questions@brettkvo.com

Rachel E. Pepper, Department of Physics, University of Puget Sound, 1500 N. Warner St., Tacoma, WA 98406, USA. Email: rpepper@pugetsound.edu

[#]Shared first authorship.

Abstract

Vorticella convallaria are microscopic sessile suspension feeders that live attached to substrates in aquatic environments. They feed using a self-generated current and help maintain the health of aquatic ecosystems and wastewater treatment facilities by consuming bacteria and detritus. Their environmental impact is mediated by their feeding rate. In ambient flow, feeding rates are highly dependent on an individual's orientation relative to the substrate and the flow. Here, we investigate how this orientation is impacted by flow speed. Furthermore, we examined whether individuals actively avoid orientations unfavorable for feeding. We exposed individuals to unidirectional laminar flow at shear rates of 0, 0.5, 1.0, and 1.5 s^{-1}, and recorded their 3D orientation using a custom biplanar microscope. We determined that *V. convallaria* orientation became progressively tilted downstream as the shear rate increased, but individuals were still able to actively reorient. Additionally, at higher shear rates, individuals spent a larger fraction of their time in orientations with reduced feeding rates. Our shear rates correspond to freestream flows on the scale of mm s^{-1} to cm s^{-1} in natural environments.

KEYWORDS
ciliate, epibiont, feeding flows, Stokeslet, suspension feeder, wastewater treatment

INTRODUCTION

In any given body of water, from ponds to streams to oceans, surface-attached microscopic organisms filter vast quantities of water as they feed.[1–5] Microscopic sessile suspension feeders (MSSFs) are single-celled protists with cell diameters ranging from a few to a few hundred microns. MSSFs feed by attaching themselves to substrates directly or with a stalk and use a self-generated current to draw in food.[6–9] Some estimates suggest that every fluid particle in some marine coastal and freshwater systems may pass through the filtering apparatus of an MSSF at least once per day.[10–13] MSSFs are prolific predators of phytoplankton and bacteria, and are common prey to larger organisms. As such, they are heavily involved in nutrient and carbon cycling, and they regulate the composition of microbial and plankton communities.[11,14,15] MSSFs are integral to aquatic ecosystems and serve as biological indicators of ecosystem health.[8,9,16,17] MSSFs are also abundant in wastewater treatment facilities and play an outsized role in clarifying effluent, with some species shown to decrease heavy metal concentrations.[18–20] They may also play a critical role in bioremediation after human-caused disasters such as oil or sewage spills.[21] The environmental impact of MSSFs is mediated by their feeding rate, which is determined by the interplay of their self-generated current and ambient flow conditions.[6,22–24]

We performed experiments on *Vorticella convallaria*, an ideal species for studying MSSFs as they are found in nearly all aquatic ecosystems, are easily cultured in the lab, and exhibit morphologies and
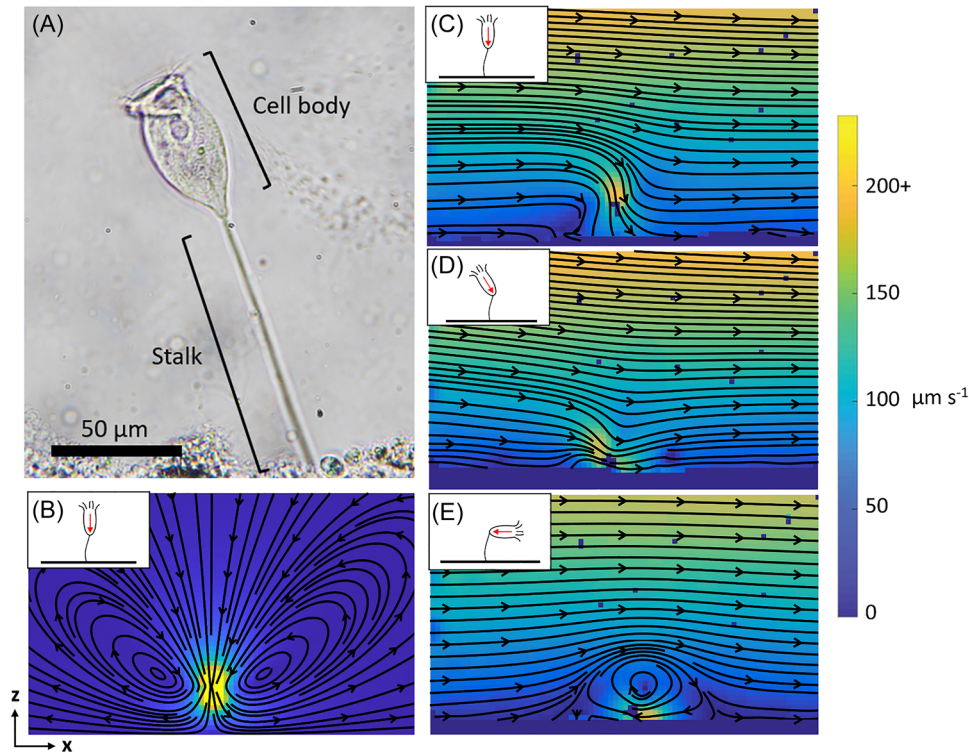
FIGURE 1 (A) *Vorticella convallaria*, a single-celled protist abundant in aquatic environments. (B) Calculated recirculating streamlines (black) in still water. *Vorticella* were modeled as a point force above a plane boundary as in Pepper et al.[24] The field of view is 2.1 × 1.3 mm. (C–E) Measured flow around *Vorticella* shows eddies when the organism is tilted downstream. Both slower net feeding flow and the presence of eddies reduce feeding rates at downstream orientations. *Vorticella* are located in the bottom middle with orientation shown in the inset. Ambient flow is from left to right following the positive x axis. The field of view is 2.1 × 1.3 mm. Figure modified from Pepper et al.[22]

behaviors that are characteristic of most other MSSF species. *Vorticella* are characteristically tulip-shaped, with a ∼100 μm stalk supporting cup-shaped bodies that exhibit a ciliated peristome (Figure 1A).[16] They draw in food with a feeding current created by rapidly beating rings of cilia around their peristome.[6,8,25,26] Their feeding current can move water at hundreds of microns per second (Figure 1B–E), allowing the *Vorticella* to directly intercept food particles within a low Reynolds number environment where viscous forces are dominant.[6,8,25,26] However, this feeding current is strongly influenced by nearby boundaries, namely, the surface to which they attach their stalk.[23,27–29] In still water, the proximity to the surface creates toroidal eddies, which recirculate water depleted of food particles through the feeding current, limiting nutrient access up to 75% (Figure 1B).[23,27–29] Calculations for no-flow conditions predict that feeding with the cell body at an angle to the substrate reduces or eliminates eddies.[24] There is evidence that *Vorticella* actively control their orientation by reorienting their cell body periodically in time with a period on the order of minutes, possibly to overcome this hydrodynamic challenge.[22,24]

While these previous findings focus on still water, MSSFs live in a diverse range of ambient flow speeds ranging from mm s^{-1} to m s^{-1} (see Table 1; for more details, see Table 1 in Pepper et al.[22]).[22,29,30] These organisms live in the viscous boundary layer, but often still experience substantial flow.[29,31,32] For unidirectional flow, it has been shown that there is a complex interplay between organism orientation,

flow direction, flow speed, and feeding rate.[22] Ambient flow enhances feeding for an individual pointed upstream and disrupts eddies in the feeding current for vertical individuals (Figure 1C,D).[22] However, for individuals tilted downstream, the feeding rate is reduced, both due to the superposition of the feeding current and ambient flow in opposite directions, and due to recirculation (Figure 1E).[22] Furthermore, individuals may be overpowered by fast-moving ambient flow and lose their ability to actively reorient. Initial 2D measurements found that individuals were tilted toward angles unfavorable for feeding as ambient flow speeds increased.[22] However, full 3D measurements are needed to confirm these observations and determine their potential impacts on feeding rates.

Here, we investigate how *V. convallaria* orientation is impacted by increasing unidirectional laminar flow speeds and whether they can actively avoid unfavorable feeding orientations. Organisms were cultured on the bottom surface of a flow chamber and exposed to unidirectional laminar flow at four speeds. The 3D orientations of 15 individuals in each flow speed were recorded for 19.5 min using a custom top- and side-view microscope. We observed that *Vorticella* were increasingly tilted downstream, with some loss of orientation ability as the flow speeds (i.e., shear rates) increased. Individuals were able to actively reorient at our highest flow speed (i.e., shear rate of 1.5 s^{-1}). Furthermore, the stalk remained more upright than the cell body, which was tilted at an angle to the flow.

TABLE 1 Calculated environmental flow speeds corresponding to experimental shear rates predicted using equations 3, 5, 8, and 10–13 from Silvester and Sleigh.[29]

Environment	Flow type	Organism location	Flow speed for 0.5 s^{-1}	Flow speed for 1.0 s^{-1}	Flow speed for 1.5 s^{-1}
Shallow stream smooth bottom (depth 10 cm)	Turbulent	Leaf or similar smooth surface	1 cm s^{-1}	1.5 cm s^{-1}	1.9 cm s^{-1}
Deep river/pond smooth bottom (depth 10 m)	Turbulent	Leaf or similar smooth surface	1.8 cm s^{-1}	2.6 cm s^{-1}	3.3 cm s^{-1}
Pebbly river (roughness 1 cm, depth 2 m)	Turbulent	Pebbly substratum	1.5 cm s^{-1}	2 cm s^{-1}	2.5 cm s^{-1}
River or stream	Laminar	Leaf or smooth surface (10 cm from leading edge)	0.6 cm s^{-1}	1 cm s^{-1}	1.3 cm s^{-1}
River or stream	Laminar	Plant stem or elongated surface parallel to flow (radius 1 mm, 10 cm from leading edge)	0.4 cm s^{-1}	0.7 cm s^{-1}	0.8 cm s^{-1}

Note: Calculated flow speeds are for freestream flows.

METHODS

We quantified the 3D kinematics of 15 individuals across four shear rates (0, 0.5, 1.0, and 1.5 s^{-1}) designed to mimic natural environments (Table 1) using a custom laminar flow chamber and custom orthogonal biplanar microscope (Figure 2A). We recorded time-lapse videos (0.333 Hz for 19.5 min) of individual *Vorticella* attached to the bottom of the flow chamber for each shear rate in a pseudo-randomized order.

Flow chamber

The internal dimensions of the flow chamber were 89 mm (L) × 9 mm (W) × 11.5 mm (H). The walls were built from 1.5-mm-thick acrylic and glued together using Weld-On #4 acrylic adhesive. The flanges on either end were built using 6.35-mm-thick acrylic. We used a soft rubber gasket to create a seal between the inner and outer flanges. We accessed the inside of the chamber by removing one or both of the flanges. The outer flanges were fitted with ⅜-inch NPT hose barbs. We found that smaller fittings resulted in the formation of eddies inside the chamber. Laser cutter files for the acrylic parts of our chamber are available in the Dryad repository associated with this article.[33]

In the bottom of the chamber, *Vorticella* were located on a 1.5-mm-thick removable acrylic slide that was held in place using thin double-sided tape intended for LCD screen repair. This slide extended the entire length of the chamber and fitted flush against the walls. We laser cut several of these slides so that we could swap them out for consecutive trials. The resulting internal height of the flow chamber was 10 mm.

The flow chamber was connected to a Harvard Apparatus PHD Model 55–1144 syringe pump outfitted with four 140-mL syringes containing diluted wheatgrass culture medium. We used ⅜-inch silicone tubing and luer-lock fittings to connect the syringes to the flow chamber. The outflow tubing was submerged in a flask of water because dripping resulted in disruption of the flow inside the chamber.

Flow measurements

We characterized the flow by tracking neutrally buoyant 11-μm hollow glass beads at nine locations throughout the chamber (three locations in the optical plane near the inlet, middle, and outlet of the chamber). We observed a typical cross-sectional parabolic flow profile and found that the flow was repeatable and laminar throughout the test section. Videos were recorded for micro-scale particle image velocimetry (μPIV) at 30 frames per second. Flow fields were determined using PIVlab software (version 2.56).[34,35] We used a single-pass PIV algorithm with interrogation windows of side length 216 pixels and step size of 108 pixels, resulting in approximately 8 hollow glass beads per window. Flow fields were then time-averaged over the length of each video (about 5 s).

We measured the shear rate by finding the velocities of particles from 0 to 580 μm above the bottom surface at nine locations across the flow chamber. At the scale of *Vorticella*, we found the velocity to vary linearly with distance from the surface. Convection was present in the no-flow condition, which caused randomly directed flow with a typical upper bound of 0.05 s^{-1}. We refer to the no-flow condition as 0 s^{-1} to indicate we did not drive flow in this condition. The syringe pump was operated with three volume flow rates: 2.6, 5.2, and 7.8 mL min^{-1}, which yielded shear rates of 0.54 ± 0.02 s^{-1}, 1.02 ± 0.03 s^{-1}, and 1.48 ± 0.04 s^{-1}. Shear rate is the rate of change in the fluid velocity from the surface to 580 μm above the surface, measured in inverse seconds. Shear rates are given as the mean ± standard error. The resulting Reynolds number (Re) in the flow chamber was 5, 9, and 14 for each condition, respectively. Here, Re = $QD/A\nu$, where Q is the volume flow rate, ν is the kinematic viscosity of water, and D and A are the hydraulic diameter and cross-sectional area of the flow chamber. Shear rates are
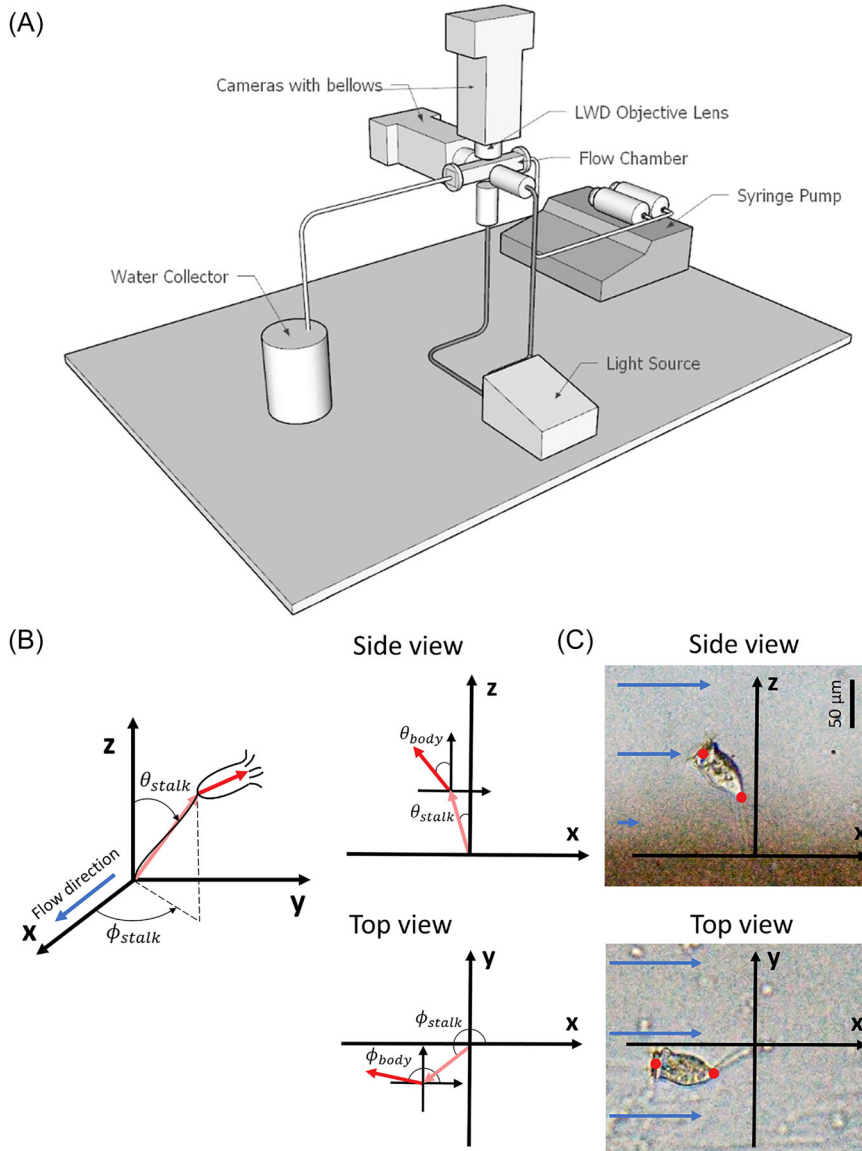
FIGURE 2 (A) Schematic of experimental setup. *Vorticella* located on the bottom of the rectangular flow chamber are recorded with a top- and side-view microscope. The flow speed is controlled with a syringe pump. (B) θ and Φ angles for the body and stalk of an example individual *Vorticella*. (C) Side and top view of an example individual *Vorticella*. Blue arrows represent flow in the +x direction. Red dots indicate points tracked in video frames to determine orientation angles for both cell body and stalk.

a reasonable first approximation of flow near surfaces, whether the surface is the floor of a rectangular chamber or the substratum exposed to flow where *Vorticella* live.[29]

Optics

Two Sony A6000 camera bodies fitted with Nikon bellows and 10× Nikon c-mount long working distance (LWD) objectives were oriented orthogonally to the flow chamber and affixed to 3-axis adjustable stages (Figure 2A). In order to fit these close to the flow chamber, the outer housing of the 10× LWD objectives was removed. Image magnification corresponded to 0.55 μm/pixel for image dimensions of 1920×1080 pixels. These cameras required an additional Sony PlayMemories timelapse add-on. The *Vorticella* were backlit using an adjustable LED light (AmScope LED-8WD Dual Spot Light) from the side and bottom (Figure 2A).

Vorticella kinematics

V. convallaria were cultured as in Vacchiano et al.[36] New colonies were created by transferring coverslips colonized by organisms to new beakers containing a wheatgrass culture media. Custom acrylic slides made to fit flush into the flow chamber were left in the culture overnight, such that several individuals colonized the slides. Once inserted into the flow chamber, *Vorticella* were located such that they were isolated from neighbors and within 25% of the maximum shear value, which occurred within 2.8 mm of the center of the channel. Individuals were simultaneously recorded from a top and side view every 3 s (0.333 Hz) for 19.5 min at each shear rate (see Video S1 for an example of these recordings). Individuals exhibited varied physical characteristics; stalk length, cell body length, and peristome diameter are listed for each in the Supporting Information. Shear rates were chosen in a pseudo-randomized order, with at least a 1-min adjustment period before the recordings were started.

Vorticella were tracked using Physlet Tracker Physics (version 6.0).[37] The origin was set where the stalk attached to the bottom surface, and two points were tracked over time: the center of the peristome (Figure 2C, upper dot) and the junction between the stalk and cell body (Figure 2C, lower dot). The side-view camera recorded coordinates in the x–z plane, while the top-view camera recorded in the x–y plane (Figure 2C). The external flow was in the $+x$ direction. The x-coordinate was taken as the average between the top-view and side-view values. Stalk angles and body angles were recorded for each video frame. The individual's stalk coordinates were given by the point tracked at the stalk-junction, while its body coordinates were given as the difference between the two points tracked. These were converted to standard spherical polar coordinates: azimuthal angle, Φ (the angle in the x–y plane with respect to the flow direction) and polar angle, θ (the angle with respect to vertical) (see Figure 2B). The polar angle, θ, indicates how much the organism is tilted from vertical. A cell body pointed directly upward from the surface (normal to the surface) has $\theta = 0°$, one pointed parallel to the surface has $\theta = 90°$, and one pointed directly down with cilia facing the surface (also normal to the surface) has $\theta = 180°$. The azimuthal angle, Φ, indicates rotation in the x–y plane (about the z-axis). It is defined for all θ angles except for $\theta = 0°$ or $180°$. At $\theta = 90°$, $\Phi = 0°$ indicates an organism aligned with the x-axis and facing directly away from the oncoming flow, while $\Phi = +/- 180°$ indicates the organism aligned with the x-axis and pointing directly into the oncoming flow. An angle of $\Phi = +/- 90°$ would be broadside to the flow aligned with the y-axis (and with the cilia pointing either in the $+$ or $-y$ direction). Since external flow was in the $+x$ direction, a completely passive cell body with no elasticity at the stalk–body junction would align with that flow, and we would predict it to have angles of $\theta = 90°$, $\Phi = 0°$. Due to the symmetry of the flow, only the value of Φ (not the sign) affects the interaction of ambient flow and *Vorticella* feeding flow. Thus, we report the absolute value of Φ (i.e., $|\Phi|$) throughout. All angles are reported as mean ± standard deviation.

Statistical analysis

The data were filtered to remove outliers resulting from spasmoneme contractions by comparing data with a moving average over five time points. Points that were more than 20% different from the moving average were replaced with the moving average. Data were assessed for normality using QQ-plots of the residuals and fitted data. We ran repeated-measures one-way ANOVAs with individual as a random effect and two-tailed post-hoc pairwise t-tests with Bonferroni-corrected p-values to assess differences between shear rates. All statistics were performed using R.[38] Our analysis code is available in a Dryad repository.[33]

Theoretical feeding rate calculation

We combined individual body angles and predictions based on the Stokeslet model in Pepper et al. to calculate theoretical feeding rates.[22]

This model determines flow velocity by combining shear flow ($u = kz$; u is horizontal flow speed, k is shear rate, and z is height from the surface) with the flow from a Stokeslet above a plane boundary (see Pepper et al., Appendix A for details of the Stokeslet flow field).[24] The Stokeslet represents the organism and pushes with a given force and given angle relative to the surface and ambient flow. The instantaneous feeding rate is determined by finding the flux of fluid in a circular area (feeding disk), which models the area the cilia can reach. By following fluid particles over time as they return to the feeding disk, this model predicts whether recirculating eddies that reduce feeding rate are present. If these eddies are present, the model predicts at what time the organism begins to feed from water that is depleted of nutrients.

Here, we matched the *Vorticella* feeding force (the Stokeslet force) to that in Pepper et al.[22] For each shear rate, we used the measured cell body angles, peristome height, and peristome width to predict the feeding rate at each time point. Since the feeding rate varies with size, we scaled each individual feeding rate by a baseline feeding rate. The baseline feeding rate was chosen as the feeding rate for the organism oriented vertically ($\theta = 0°$). Baseline feeding rates are listed for each individual in the Supporting Information. We then found the time-averaged scaled feeding rate for each individual at each shear rate. An example of how scaled feeding rate varies with orientation and shear rate is shown in Figure 3. We also determined what angles led to recirculation in the flow (outlined in white in Figure 3), and ultimately what percent of the time each individual spent in an orientation that would lead to recirculation (i.e., orientations that had eddies in the flow that intersected the feeding disk).

RESULTS

Vorticella cell bodies and stalks were increasingly pushed downstream as the shear rate increased. Individuals were capable of actively reorienting both their bodies and stalks at all shear rates, although we sometimes observed maximum amplitudes of these movements were diminished at higher shear rates. The most typical behavior was a circular rotation or arc with a period on the order of several minutes (e.g., Figure 4, individuals 1 and 2), similar to previous observations.[22,24] However, we also observed more sporadic behavior in some individuals (Figure 4, individual 3). As the shear rate increased, we expected individuals to be influenced by drag and shift toward body angles of $\theta = 90°$ and $\Phi = 0°$. We also expected that at some shear rates they would lose the ability to actively reorient. Instead, at every shear rate, we observed individuals were capable of actively reorienting over time. Angle versus time figures similar to Figure 4 are available for all individuals in the Supporting Information, and both our raw and filtered data are available through the Dryad repository.[33]

We averaged time-course data for each individual at each shear rate to get typical orientation angles. We took the root mean square (RMS) of the time-course data for each individual at each shear rate as a measure of oscillation amplitude (we first subtracted the mean angle for each set of time course data before calculating the RMS, to better approximate an amplitude). We then compared both the mean angle
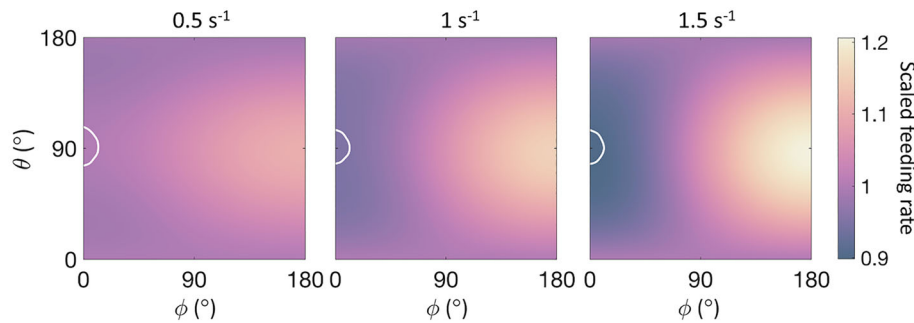
FIGURE 3 Calculated feeding rates (shown as different colors) as a function of cell body orientation for three different shear rates. Feeding rates are scaled by the feeding rate at $\theta = 0°$, which does not change with ambient flow. White lines outline the angles where eddies occur in the flow near the organism and there is recirculation through the feeding disk. These angles are determined separately from feeding rate, and are centered on $\theta = 90°$, $\Phi = 0°$. The illustrative feeding rates and recirculation zones shown here were calculated for an organism with a peristome 109 µm above the surface of attachment, the average value over all our measurements, and with a representative peristome radius of one tenth this height. Angles leading to recirculation were taken directly from the calculation shown here, while scaled feeding rates for individuals were calculated using measured peristome heights and widths.

and RMS across all 15 individuals (Figures 5 and 6). We also combined all time points for all individuals to make histograms of the percent time *Vorticella* were observed at all possible orientations (all θ and Φ combinations; Figure 7).

At all shear rates, there was wide variation in mean $|\Phi|$ and θ across individuals (Figure 5). As shear rates increased, variation in average orientation across all individuals decreased for body and stalk $|\Phi|$ but not for θ (Figure 5). We also observed that individuals spent more time with azimuthal angles close to $\Phi = 0°$ as shear rate increased (Figures 5A,B and 7A,B). On the other hand, the RMS in amplitude for an individual organism over time (i.e., the RMS of its oscillations) did not change for body or stalk $|\Phi|$ and θ with increasing shear rates (Figure 6). These observations together indicate that: (1) individuals were pushed downstream as shear rate increased, and (2) individuals maintained active control over their oscillations with similar amplitudes across all shear rates.
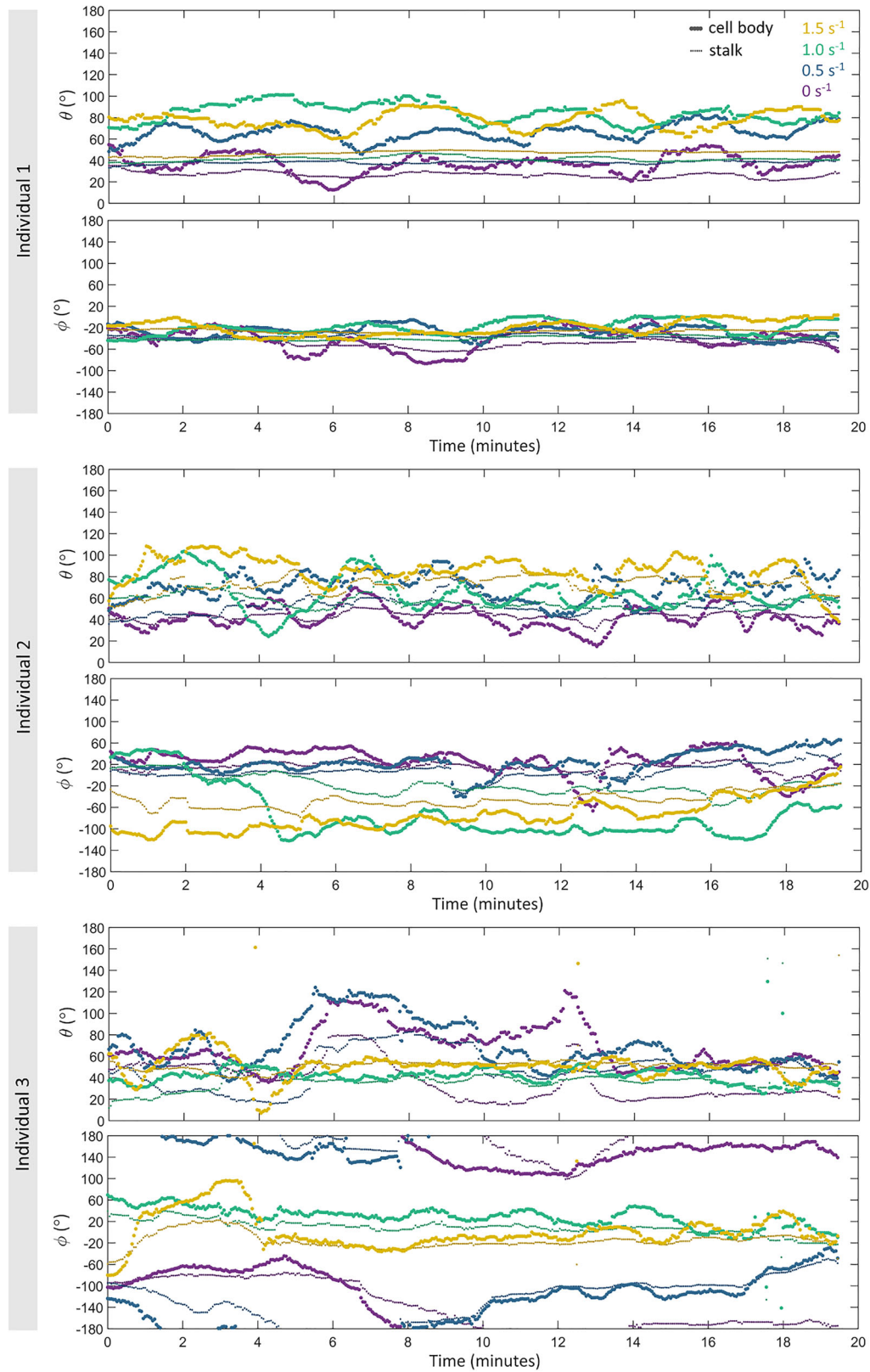
Cell body orientation

Cell body $|\Phi|$ decreased with increasing shear rate (i.e., angled more downstream azimuthally and aligned more closely with the direction of flow ($F(3,42) = 5.164$, $p = 0.004$, Figure 5A). Post-hoc tests showed a significant difference between 0 and 1.5 s^{-1} after correcting for multiple tests ($t(14) = 3.44$, $p = 0.02$, 95% C.I. = [13.90, 60.05], Bonferroni-corrected, Figure 5A). The typical cell body angles were rotated downstream azimuthally, such that the average angle at 1.5 s^{-1} was $|\Phi| = 35° \pm 31°$. The *Vorticella* maintained a typical cell body θ of $53° \pm 19°$ regardless of flow speed ($F(3,42) = 2.114$, $p = 0.113$, Figure 5C); however, there is a slight trend toward higher angles (i.e., more tilted from the vertical) at higher shear rates. This indicates that as flow speed increased, the typical angle was not further tilted down vertically, but did rotate in the x–y plane to align more with the flow. The oscillation amplitudes in θ and Φ decreased slightly as shear rates increased; however, this trend was not significant (Figure 6A,C, $p > 0.1$ for both).
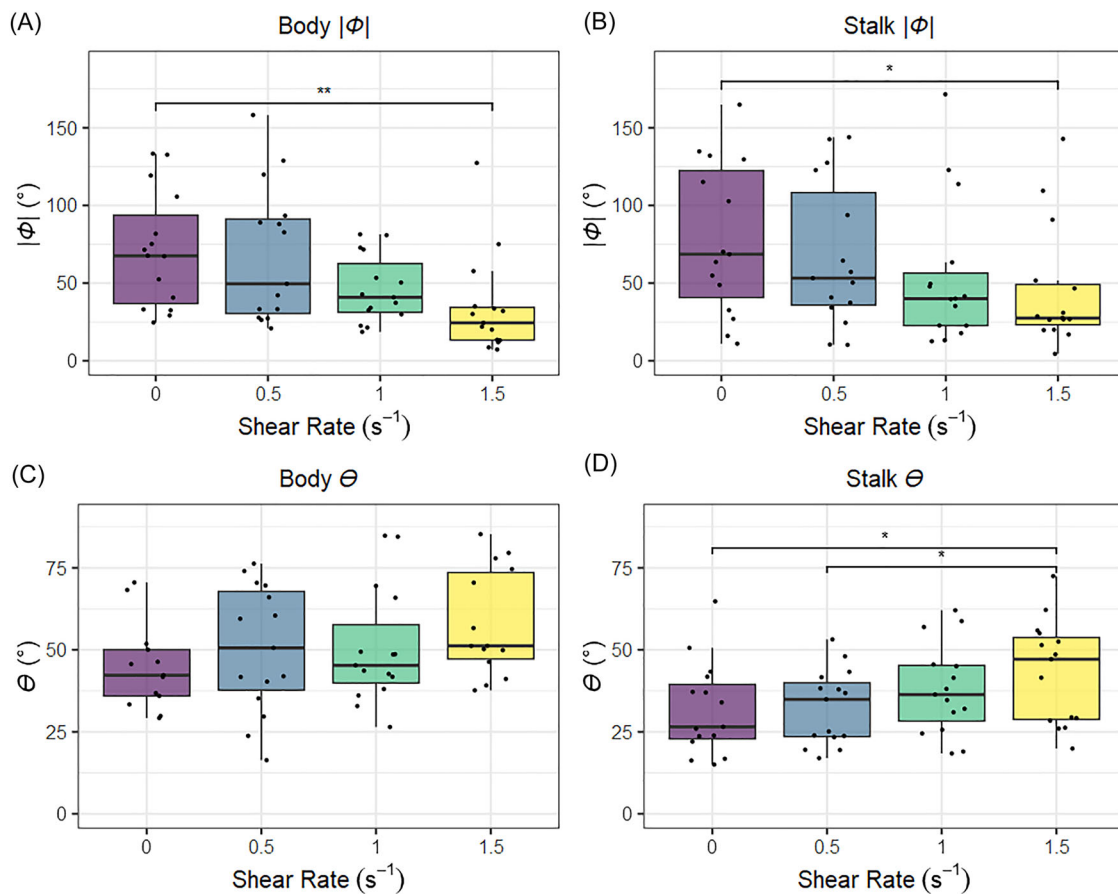
Stalk orientation

Stalk $|\Phi|$ decreased significantly with increasing shear rate ($F(3,42) = 5.906$, $p = 0.002$, Figure 5B). Post-hoc tests showed significant differences between 0 and 1.5 s^{-1} after correcting for multiple tests ($t(14) = 12.2$, $p = 0.027$, 95% C.I. = [12.2, 54.8], Bonferroni-corrected, Figure 5B). Stalk θ was significantly different across shear rates ($F(3,42) = 6.387$, $p = 0.01$, Figure 5D), with a general trend toward increased angles at higher shear rates. Post-hoc tests showed differences in stalk θ between 0 and 1 s^{-1} ($t(14) = -3.34$, $p = 0.029$, 95% C.I. = [−18.3,−3.98], Bonferroni-corrected, Figure 5D), and 0.5 and 1.5 s^{-1} ($t(14) = -3.61$, $p = 0.017$, 95% C.I. = [−17.0,−4.33], Bonferroni-corrected, Figure 5D). This indicates that as flow increased, the stalk was both tilted down vertically toward the horizontal and rotated to align with the direction of flow. The stalk oscillation amplitudes in θ and Φ also decreased slightly as shear rates increased (Figure 6B,D). For Φ, there was a significant difference when comparing across all groups ($F(3,42) = 3.039$, $p = 0.039$, Figure 6B), but after correcting for multiple comparisons, this effect was lost ($p > 0.05$ for all, Bonferroni-corrected, Figure 6B). There were no significant differences in θ across shear rate ($F(3,42) = 3.039$, $p = 0.101$, Figure 6D).

Theoretical feeding rate

As the shear rate increased, the calculated feeding rate significantly decreased ($F(3,42) = 12.67$, $p < 0.001$, Figure 8A). In the no-flow condition, the mean scaled feeding rate was 0.97 ± 0.09, while at the highest shear rate of 1.5 s^{-1}, it was reduced to 0.85 ± 0.10 (Figure 8A). This result is a combination of two effects associated with increased shear rates: (1) individuals spent more time pointed downstream (Figures 5 and 7), and (2) feeding rate was reduced across a wider range of angles due to superposition of opposing feeding and ambient flows (Figure 3). Post-hoc tests showed differences in theoretical feeding rate between 0 and 1.5 s^{-1} ($t(14) = 3.58$, $p = 0.018$, 95% C.I. = [0.048, 0.190], Bonferroni-corrected), 0.5 and 1 s^{-1} ($t(14) = 3.39$, $p = 0.026$, 95%

FIGURE 4   Orientation over time for three representative *V. convallaria* individuals. Bold lines show cell body orientation, while thin lines show stalk orientation. Each dot corresponds to a raw data point recorded at 0.333 Hz. Outlier data points (e.g., individual 3 at 18 min, shear 1.0 s⁻¹) represent organism contractions and have been excluded in filtered data. Shear rate is indicated by color. Angle versus time figures similar to Figure 4 are available for all individuals in the Supporting Information, and both our raw and filtered data are available through our Dryad repository.[33]

FIGURE 5 Typical body and stalk angles change with flow speed. Increasing shear rate resulted in downstream reorientation of both cell body and stalk. The bar is the median of the typical angle (averaged over time) of each individual ($n = 15$). The box indicates interquartile range (IQR), and the whiskers show the IQR $\times$ 1.5. The average angle for each individual is plotted using dots. Panel (A) is cell body $|\Phi|$, (B) is stalk $|\Phi|$, (C) is cell body θ, and (D) is stalk θ. *$p < 0.05$; **$p < 0.01$.

C.I. = [0.015, 0.067], Bonferroni-corrected), and 0.5 and 1.5 s^{-1} ($t(14)$ = 5.23, $p < 0.001$, 95% C.I. = [0.070, 0.166], Bonferroni-corrected).

On the other hand, we found that most *Vorticella* spent very little time in orientations that led to recirculation, even at the highest shear rates. At 1.5 s^{-1}, one individual spent 65% of its time at angles that lead to recirculation. Most individuals spent zero or nearly zero percent of their time in orientations that would cause recirculation. Additionally, since an individual must stay in recirculating flow for some time before it depletes the available food, our results suggest that recirculation does not restrict feeding for *Vorticella* at the flow rates we examined.[39]

DISCUSSION

Flow reduces theoretical feeding rate

Our results show that increased shear flow pushed *V. convallaria* toward orientations that were unfavorable for feeding. Both the cell body and the stalk were angled downstream; however, they maintained their ability to actively rotate. Thus, at the highest shear rate, 1.5 s^{-1}, the average theoretical feeding rate was 12% lower than the average

theoretical feeding rate in no flow. This reduction is relevant on both ecological and individual scales: a 12% reduction of nutrient uptake is significant for growth and reproduction. Furthermore, a reduction in the clearance rate of bacteria and detritus in an environment of that magnitude could result in changes to entire ecosystems. It is somewhat surprising that we saw such a reduction in theoretical feeding rate given that the flow speeds used here are quite slow compared to flows in many natural environments. The flows tested here correspond to bodies of water with freestream flows on the order of millimeters per second to centimeters per second (Table 1). These flow speeds are found in slow-moving streams and rivers, ponds, puddles, and around sinking marine snow. The sinking aggregates that comprise marine snow are common attachment sites for MSSFs.[40] These aggregates have been shown to settle at on the order of mm s^{-1}.[30]

In freestream flows on the scale of tens of centimeters per second to meters per second, typical for many rivers and streams, feeding rates of *Vorticella* are likely to be further reduced. Individuals that experience these flows are almost certainly forced further toward orientations that result in poor feeding rates, and in faster flows likely lose the ability to actively reorientate altogether. Risse-Buhl et al.[41] exposed *V. convallaria* to fast flows in a petri dish, and found that the stalks were tilted
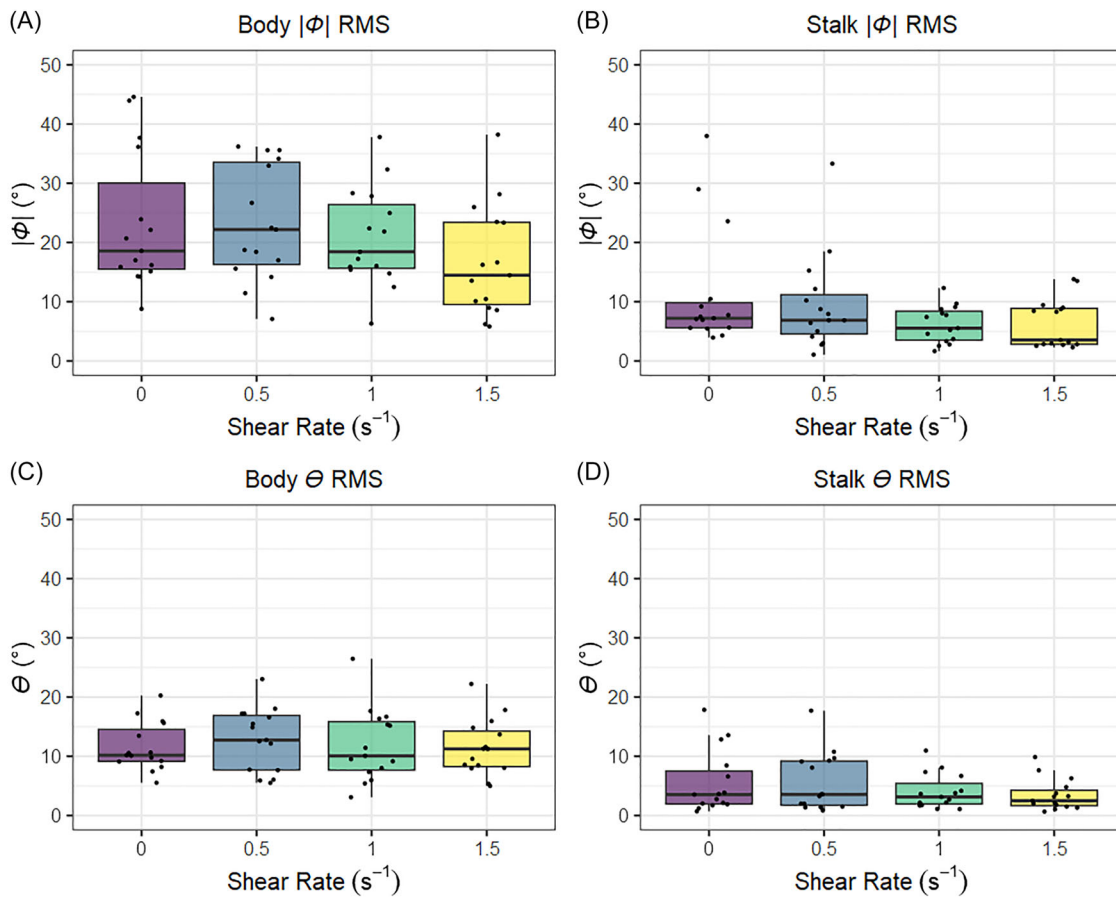
FIGURE 6 Variation in angle across shear rates. Generally, there is less variation in stalk than body and less variation in θ than Φ. Each panel shows the root mean square (RMS) of angle for each shear rate, which serves as a proxy for oscillation amplitude. The bar is the median of the RMS values of each individual ($n = 15$). The box indicates interquartile range (IQR), and the whiskers show the IQR × 1.5. The measured RMS for each individual is plotted as small dots. Panel (A) is cell body $|\Phi|$, (B) is stalk $|\Phi|$, (C) is cell body θ, and (D) is stalk θ.
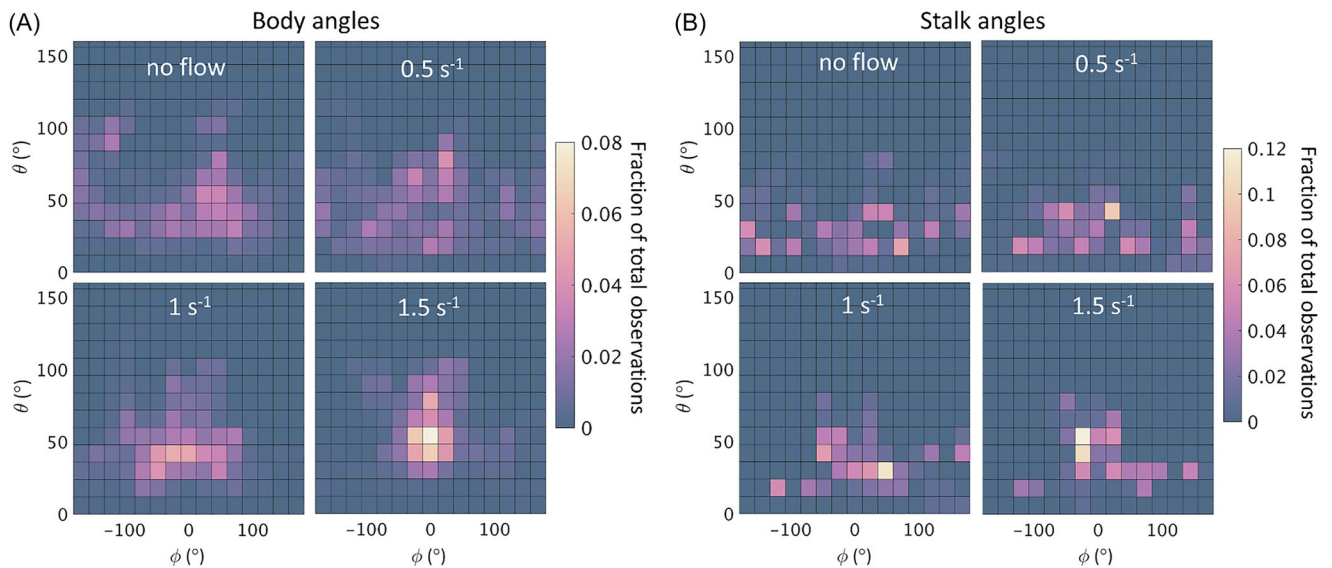
FIGURE 7 Heatmap histogram of orientation across shear rates. As the shear rate increased, body and stalk angles were increasingly pointed downstream. (A) is cell body orientation, and (B) is stalk orientation. Colors indicate the frequency of each θ/Φ combination observed across all time points, all individuals, and all shear rates. Frequencies are reported as a fraction of the total number of time points observed. Note that the color scale is different between panels (A) and (B), as there was less variation in stalk angles as compared to body angles overall.
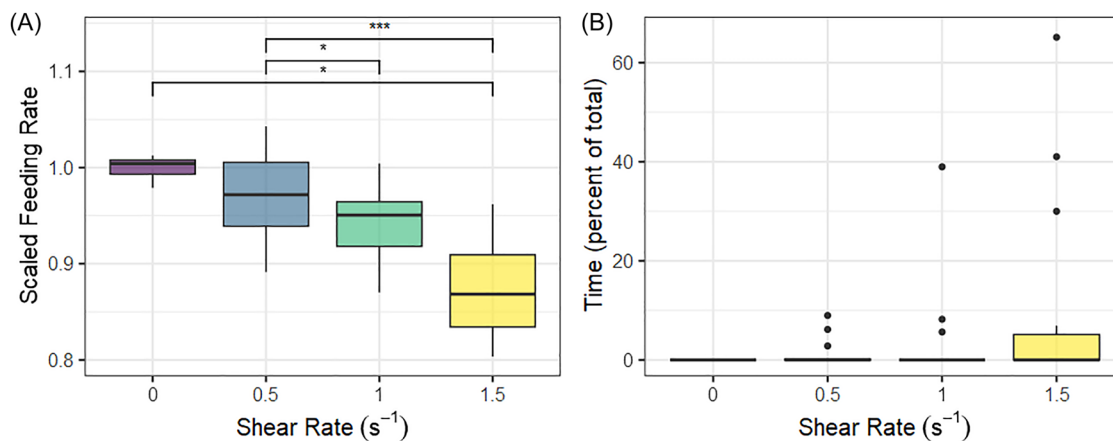
FIGURE 8 (A) Calculated scaled feeding rate decreases with increasing shear rate. (B) Calculated percent of time spent in recirculation is always near zero and does not change with shear rate. $*p < 0.05$; $***p < 0.001$.

so that the organisms were "lying on the surface," but the cell body orientation was not measured (we estimate that their flow speeds correspond to shear rates of approximately $10\,\mathrm{s}^{-1}$ based on their Figure 1). It is a clear area for future work to perform similar experiments to ours at higher flow speeds up until the loss of active control is observed.

At these high flow speeds, *Vorticella* likely lose the ability to feed completely, eliminating these environments as potential habitats. We can use a scaling analysis to determine the approximate shear rate when this happens and predict in what environments they occur. To do this, we compare the torque on the cell body to the torque the organisms are able to exert with their cilia. The torque on a sphere in simple shear flow is approximately $4\pi a^3 \mu k$, where a is the radius of the sphere, μ the viscosity of the water, and k the shear rate.[42] The approximate torque that the *Vorticella* can apply to its cell body relative to the junction with the stalk is $2fa$, where f is the force applied by the cilia to the surrounding water. The *Vorticella* will lose the ability to reorient when its torque equals the torque from the shear flow, so we find that *Vorticella* are able to reorient when $k \leq \frac{f}{2\pi a^2 \mu}$. Using parameters from Pepper et al.[22] ($f = 230\,\mathrm{pN}$ and $a = 25\,\mu\mathrm{m}$), we predict that *Vorticella* lose the ability to control their orientation for shear rates on the order of $10\,\mathrm{s}^{-1}$, a factor of 10 greater than our experiments. This corresponds to environmental flows of around $5\,\mathrm{cm\,s}^{-1}$ to $1\,\mathrm{m\,s}^{-1}$, depending on the details of the substrate geometry and the flow environment.[29]

Habitat selection

Indeed, there is evidence that *Vorticella* and other stalked sessile ciliates are found more abundantly in bodies of water with slower flow, though this has been studied in only a few habitats. Baldock found a negative correlation between flow speed in a stream and the abundance of *Vorticella* and other ciliates on aquatic plant surfaces.[29,43] While *Vorticella* were abundant on leaves of aquatic vegetation during low-flow conditions in a brook with moderate flow, a faster-flowing river had only very few *Vorticella* on similar leaf surfaces. Sessile ciliates, including *Vorticella* species, were also found to be more abundant

in areas with slower flow in both laboratory experiments (rectangular channels with flow velocity ranging from 5 to $80\,\mathrm{cm\,s}^{-1}$) and on biofilms in streams (9 to $32\,\mathrm{cm\,s}^{-1}$).[44]

This change in abundance with flow speed could be due to differential colonization rates, or to *Vorticella* leaving when flow speed becomes too high for them. *Vorticella* detach from their stalk and transform to a free-swimming telotroph form when environmental conditions are unfavorable.[16,45–47] Increased freestream flow leads to increased detachment of *Vorticella*, and, further, after large storms with very high flow speeds, there are mass-detachment events where many *Vorticella* transform to the free-swimming form.[16,48] While it has been hypothesized that these mass-detachments occur to take advantage of storms as a population dispersal mechanism, our results indicate that *Vorticella* may detach because these higher flows restrict feeding.[16]

Even in environments with very high flow speeds, *Vorticella* and other stalked MSSFs may be able to take advantage of sheltered areas. There is evidence that surface topography that slows flow can lead to increased abundance of heterotrophic nanoflagellates.[49] Moreover, ciliates have been found to be more abundant in the protected nodes of plants.[50] Both ciliates and nanoflagellates are also present in pores within the upper layers of the sediment at the bottom of streams and rivers where flow is significantly slower than at the sediment surface.[51]

Anthropogenic disturbances that alter aquatic habitats likely affect the distribution and abundance of MSSFs. For instance, humans have channelized many rivers, which can increase overall flow speed, thereby reducing the habitat available to MSSFs. Changes in mountain rain and snowfall due to climate change also cause changes in flow speed in rivers and streams that could impact MSSFs, as well as other aquatic organisms.[52]

Wastewater treatment facilities

Microorganisms play an essential role in the clarification of wastewater effluent. MSSFs are a useful indicator species of the quality of activated sludge, and exist throughout the wastewater treatment process.[53]

Vorticella are most commonly found in the aeration tanks and secondary clarifiers, where they colonize the biofilm and remove organic waste under aerobic conditions.[54] In one study, 14% of the water was cleared by the filter-feeding of *Epistylis*, a ciliate similar to *Vorticella*.[55] Engineers aiming to maximize the performance of these filter feeders should consider the ambient flow speeds of these wastewater treatment stages during their design. Trickle filters and rotating biological contactors are regularly employed to maximize surface area such that MSSFs can flourish.[56] These systems could possibly be improved through investigation of the flow characteristics at the scale of MSSFs.

Flow that is not unidirectional

This work focuses on unidirectional laminar flow, which is only one of many typical flow conditions experienced in nature. If the flow pulses or changes direction, *Vorticella* may be able to feed more effectively. For instance, coral tentacles move out of phase in oscillatory flow due to their elasticity.[57] Similarly, MSSFs experiencing oscillatory flow could spend a significant amount of time facing into the flow. This could also happen in flows that change direction randomly, such as boundary layer flow driven by turbulence. It would, therefore, be interesting to study *Vorticella* response to such flows in the lab and in their natural habitats.

Implications for the reorientation mechanism

This work clearly shows that *V. convallaria* actively reorient their cell body periodically in time.[24] Neither the mechanism nor underlying benefit of this motion is well understood. Our results have some implications for both of these questions.

The periodic reorientation of the cell body could be driven by the cilia as they push the fluid and create the feeding current, or they could be driven by some kind of actuator at the body–stalk junction. Our analysis of the ciliary force in the above section on feeding implications indicates that the force exerted by the cilia on the water is strong enough to drive reorientation against the shear flow in our experiments. While this does not rule out an actuator at the stalk junction, there is also no evidence of any such motile structures in this region that we are aware of (the structure has been studied in the context of detachment/attachment of the stalk, but not in this context as far as we know).[47] Our results show that individual organisms usually reorient periodically around a typical angle or base angle and that this base angle varies widely among individuals (Figures 4 and 5). We hypothesize that this base angle may be set by passive structures at the stalk junction that also have some stiffness that resists change to this angle. The cilia then actively drive oscillations around this base angle.

Individuals exhibited a smaller range of typical θ angles than Φ angles and smaller oscillations around θ than Φ, and maintained these as flow speed increases (Figures 5 and 6). This may indicate either a stronger mechanism of control in the θ direction or some stronger advantage to the organism for maintaining a particular polar orien-

tation versus azimuthal orientation. Tilting down from the vertical, while simultaneously exploring a range of azimuthal angles could be an effective strategy for maximizing nutrient uptake if food comes unpredictably from all directions. It is also an effective method to reduce the impact of recirculation by rotating regularly: Individuals that encounter momentary recirculatory flow will not exhaust the available food in the entrained eddy before they exit the recirculation.

It is also known that the cilia beat primarily in the polar direction, with only a small azimuthal component, and flow is not driven azimuthally for *Vorticella*.[6] This also supports a hypothesis that *Vorticella* can exert more control over orientation in the polar orientation without extensive disruption to the regular ciliary beat patterns exhibited during feeding.

Our results are also consistent with the cell body being active while the stalk is completely passive for the reorientations that we observe. This is indicated by our observations that individual variation is less for stalk than body angles (Figure 6), showing that oscillation of the body could be driving stalk oscillations. It is further supported by our observation that the typical stalk angles are more affected by flow than typical body angles. The flow could be pushing the whole body, which continues to reorient, while the stalk responds passively to the drag force of the fluid pushing the cell body in the direction of flow.

CONCLUSION

Here, we observed that *V. convallaria* orientation was affected by ambient fluid flow, and that relatively slow unidirectional flow pushed individuals into orientations with theoretically reduced feeding rates. These reductions are significant to both individual fitness and the impact of a population of these organisms on the environment. We predict that in faster flows organisms with flexible stalks like *V. convallaria* will be pushed into orientations where they are unable to feed effectively. Our results also show that *V. convallaria* exerted more control over their polar angle than their azimuthal angle. We also show that it is possible that all active motion of *V. convallaria* is driven by the cilia, but we do not rule out other actuators.

analysis and thoughtful discussion, and Sangjin Ryu for *V. convallaria* cultures and helpful advice on culture maintenance.

ORCID

Brett Klaassen van Oorschot https://orcid.org/0000-0003-4347-5391

Rachel E. Pepper https://orcid.org/0000-0001-6804-8965

REFERENCES

1. Dopheide, A., Lear, G., Stott, R., & Lewis, G. (2009). Relative diversity and community structure of ciliates in stream biofilms according to molecular and microscopy methods. *Applied and Environmental Microbiology*, *75*, 5261–5272. https://doi.org/10.1128/AEM.00412-09

2. Taylor, W. D. (1983). A comparative study of the sessile, filter-feeding ciliates of several small streams. *Hydrobiologia*, *98*, 125–133. https://doi.org/10.1007/BF02185630

3. Kankaala, P., & Eloranta, P. (1987). Epizooic ciliates (*Vorticella* sp.) compete for food with their host *Daphnia longispina* in a small polyhumic lake. *Oecologia*, *73*, 203–206. https://doi.org/10.1007/BF00377508

4. Sieburth, J. M. (1984). Protozoan bacterivory in pelagic marine waters. In J. E. Hobbie, & P. J. I. Williams (Eds.). *Heterotrophic activity in the sea* (pp. 405–444). Springer US. https://doi.org/10.1007/978-1-4684-9010-7_18

5. Carrias, J.-F., Amblard, C., & Bourdier, G. (1996). Protistan bacterivory in an oligomesotrophic lake: Importance of attached ciliates and flagellates. *Microbial Ecology*, *31*, 249–268. https://doi.org/10.1007/BF00171570

6. Sleigh, M. A., & Barlow, D. (1976). Collection of food by vorticella. *Transactions of the American Microscopical Society*, *95*, 482–486. https://doi.org/10.2307/3225140

7. Higdon, J. J. L. (1979). The generation of feeding currents by flagellar motions. *Journal of Fluid Mechanics*, *94*, 305–330. https://doi.org/10.1017/S002211207900104X

8. Fenchel, T. (1986). Protozoan filter feeding. *Progress in Protistology*, *1*, 65–113.

9. Fenchel, T. (1980). Suspension feeding in ciliated protozoa: Feeding rates and their ecological significance. *Microbial Ecology*, *6*, 13–25. https://doi.org/10.1007/BF02020371

10. Leadbeater, B. S. C., & Green, J. C. (2014). *Flagellates: Unity, diversity and evolution*. CRC Press. https://doi.org/10.1201/9781482268225

11. Boenigk, J., & Arndt, H. (2002). Bacterivory by heterotrophic flagellates: Community structure and feeding strategies. *Antonie Van Leeuwenhoek*, *81*, 465–480. https://doi.org/10.1023/A:1020509305868

12. Fenchel, T. (1987). *Ecology of protozoa*. Springer. https://doi.org/10.1007/978-3-662-06817-5

13. Boenigk, J., & Arndt, H. (2000). Particle handling during interception feeding by four species of heterotrophic nanoflagellates. *Journal of Eukaryotic Microbiology*, *47*, 350–358. https://doi.org/10.1111/j.1550-7408.2000.tb00060.x

14. Sherr, E. B., & Sherr, B. F. (2002). Significance of predation by protists in aquatic microbial food webs. *Antonie Van Leeuwenhoek*, *81*, 293–308. https://doi.org/10.1023/a:1020591307260

15. Sherr, E. B., & Sherr, B. F. (1994). Bacterivory and herbivory: Key roles of phagotrophic protists in pelagic food webs. *Microbial Ecology*, *28*, 223–235. https://doi.org/10.1007/BF00166812

16. Buhse, H. E., McCutcheon, S. M., Clamp, J. C., & Sun, P. (2011). Vorticella. In *Encyclopedia of life sciences*. John Wiley & Sons, Ltd. https://doi.org/10.1002/9780470015902.a0001975.pub2

17. Azam, F., Fenchel, T., Field, J., Gray, J., Meyer-Reil, L., & Thingstad, F. (1983). The ecological role of water-column microbes in the sea. *Marine Ecology Progress Series*, *10*, 257–263. https://doi.org/10.3354/meps010257

18. Rehman, A., Shakoori, F. R., & Shakoori, A. R. (2010). Resistance and uptake of heavy metals by *Vorticella microstoma* and its potential use in industrial wastewater treatment. *Environmental Progress & Sustainable Energy*, *29*, 481–486. https://doi.org/10.1002/ep.10450

19. Reid, R. (1969). Fluctuations in populations of 3 vorticella species from an activated-sludge sewage plant. *Journal of Protozoology*, *16*, 103–111. https://doi.org/10.1111/j.1550-7408.1969.tb02240.x

20. Fried, J., & Lemmer, H. (2003). On the dynamics and function of ciliates in sequencing batch biofilm reactors. *Water Science Technology*, *47*, 189–196.

21. Gertler, C., Näther, D. J., Gerdts, G., Malpass, M. C., & Golyshin, P. N. (2010). A mesocosm study of the changes in marine flagellate and ciliate communities in a crude oil bioremediation trial. *Microbial Ecology*, *60*, 180–191. https://doi.org/10.1007/s00248-010-9660-3

22. Pepper, R. E., Riley, E. E., Baron, M., Hurot, T., Nielsen, L. T., Koehl, M. A. R, Kiørboe, T., & Andersen, A. (2021). The effect of external flow on the feeding currents of sessile microorganisms. *Journal of the Royal Society Interface*, *18*, 20200953. https://doi.org/10.1098/rsif.2020.0953

23. Hartmann, C., Karslioglu, Ö., Petermeier, H., Fried, J., & Delgado, A. (2007). Analysis of the flow field induced by the sessile peritrichous ciliate *Opercularia asymmetrica*. *Journal of Biomechanics*, *1*, 137–148.

24. Pepper, R. E., Roper, M., Ryu, S., Matsumoto, N., Nagai, M., & Stone, H. A. (2013). A new angle on microscopic suspension feeders near boundaries. *Biophysics Journal*, *105*, 1796–1804. https://doi.org/10.1016/j.bpj.2013.08.029

25. Ryu, S., Pepper, R. E., Nagai, M., & France, D. C. (2016). Vorticella: A protozoan for bio-inspired engineering. *Micromachines*, *8*, 4. https://doi.org/10.3390/mi8010004

26. Nagai, M., Oishi, M., Oshima, M., Asai, H., & Fujita, H. (2009). Three-dimensional two-component velocity measurement of the flow field induced by the *Vorticella picta* microorganism using a confocal microparticle image velocimetry technique. *Biomicrofluidics*, *3*, 014105. https://doi.org/10.1063/1.3105106

27. Pepper, R. E., Roper, M., Ryu, S., Matsudaira, P., & Stone, H. A. (2010). Nearby boundaries create eddies near microscopic filter feeders. *Journal of the Royal Society Interface*, *7*, 851–862. https://doi.org/10.1098/rsif.2009.0419

28. Liron, N., & Blake, J. R. (1981). Existence of viscous eddies near boundaries. *Journal of Fluid Mechanics*, *107*, 109–129. https://doi.org/10.1017/S0022112081001699

29. Silvester, N. R., & Sleigh, M. A. (1985). The forces on microorganisms at surfaces in flowing water. *Freshwater Biology*, *15*, 433–448. https://doi.org/10.1111/j.1365-2427.1985.tb00213.x

30. Alldredge, A. L., & Gotschalk, C. (1988). In situ settling behavior of marine snow. *Limnology and Oceanography*, *33*, 339–351. https://doi.org/10.4319/lo.1988.33.3.0339

31. Shimeta, J., Starczak, V., Ashiru, O., & Zimmer, C. (2001). Influences of benthic boundary-layer flow on feeding rates of ciliates and flagellates at the sediment-water interface. *Limnology and Oceanography*, *46*, 1709–1719. https://doi.org/10.4319/lo.2001.46.7.1709

32. Grünbaum, D. (1995). A model of feeding currents in encrusting bryozoans shows interference between zooids within a colony. *Journal of Theoretical Biology*, *174*, 409–425. https://doi.org/10.1006/jtbi.1995.0108

33. Pepper, R., Klaassen van Oorschot, B., & Böttger, T. (2023). Data from: The effect of external flow on 3D orientation of a microscopic sessile suspension feeder, *Vorticella convallaria*. https://doi.org/10.5061/dryad.7d7wm3829

34. Thielicke, W., & Sonntag, R. (2021). Particle Image Velocimetry for MATLAB: Accuracy and enhanced algorithms in PIVlab. *Journal of Open Research Software*, 9, 12. https://doi.org/10.5334/jors.334

35. Thielicke, W., & Stamhuis, E. J. (2014). PIVlab—Towards user-friendly, affordable and accurate digital Particle Image Velocimetry in MATLAB. *Journal of Open Research Software*, 2, e30. https://doi.org/10.5334/jors.bl

36. Vacchiano, E. J., Kut, J. L., Wyatt, M. L., Buhse, H. E. J., Vacchiano, E. J., Kut, J. L., Wyatt, M. L., & Buhse, H. E. J. (1991). A novel method for mass culturing vorticella. *Journal of Protozoology*, 38, 608–613.

37. Brown, D., Hanson, R., & Christian, W. (2021). Tracker video analysis and modeling tool.

38. R Core Team. (2023). R: A language and environment for statistical computing. Vienna, Austria: R Foundation for Statistical Computing. https://www.R-project.org

39. Rode, M., Meucci, G., Seegert, K., Kiørboe, T., & Andersen, A. (2020). Effects of surface proximity and force orientation on the feeding flows of microorganisms on solid surfaces. *Physical Review Fluids*, 5, 123104. https://doi.org/10.1103/PhysRevFluids.5.123104

40. Jonsson, P. R., Johansson, M., & Pierce, R. W. (2004). Attachment to suspended particles may improve foraging and reduce predation risk for tintinnid ciliates. *Limnology and Oceanography*, 49, 1907–1914. https://doi.org/10.4319/lo.2004.49.6.1907

41. Risse-Buhl, U., Scherwass, A., Schlüssel, A., Arndt, H., Kröwer, S., & Küsel, K. (2009). Detachment and motility of surface-associated ciliates at increased flow velocities. *Aquatic Microbial Ecology*, 55, 209–218. https://doi.org/10.3354/ame01302

42. Chaoui, M., & Feuillebois, F. (2003). Creeping flow around a sphere in a shear flow close to a wall. *Quarterly Journal of Mechanics and Applied Mathematics*, 56, 381–410. https://doi.org/10.1093/qjmam/56.3.381

43. Baldock, B. M. (1980). The ecology of protozoa in chalk streams, with particular reference to ciliates and amoebae associated with selected macrophytes. University of Southampton, Doctoral Thesis.

44. Risse-Buhl, U., & Küsel, K. (2009). Colonization dynamics of biofilm-associated ciliate morphotypes at different flow velocities. *European Journal of Protistology*, 45, 64–76. https://doi.org/10.1016/j.ejop.2008.08.001

45. Vacchiano, E., Dreisbach, A., Locascio, D., Castaneda, L., Vivian, T., & Buhse, H. E. (1992). Morphogenetic transitions and cytoskeletal elements of the stalked zooid and the telotroch stages in the peritrich ciliate *Vorticella convallaria*. *Journal of Protozoology*, 39, 101–106. https://doi.org/10.1111/j.1550-7408.1992.tb01288.x

46. Baufer, P. J. D., Pylawka, S., & Buhse, H. E. (2000). Evidence for a signal transduction system initiating stalk excision in *Vorticella convallaria*. *Transactions of the Illinois State Academy of Science*, 93, 201–213.

47. Wibel, R., Vacchiano, E., Maciejewski, J., Buhse, H., & Clamp, J. (2007). The fine structure of the scopula-stalk region of *Vorticella convallaria*. *Journal of Eukaryotic Microbiology*, 44, 457–466. https://doi.org/10.1111/j.1550-7408.1997.tb05724.x

48. Kusuoka, Y., & Watanabe, Y. (1987). Growth and survival of peritrich ciliates in an urban stream. *Oecologia*, 73, 16–20. https://doi.org/10.1007/BF00376971

49. Willkomm, M., Schlüssel, A., Reiz, E., & Arndt, H. (2007). Effects of microcurrents in the boundary layer on the attachment of benthic heterotrophic nanoflagellates. *Aquatic Microbial Ecology*, 48, 169–174. https://doi.org/10.3354/ame048169

50. Baldock, B. M., Baker, J. H., & Sleigh, M. A. (1983). Abundance and productivity of protozoa in chalk streams. *Ecography*, 6, 238–246. https://doi.org/10.1111/j.1600-0587.1983.tb01087.x

51. Cleven, E.-J. (2004). Seasonal and spatial distribution of ciliates in the sandy hyporheic zone of a lowland stream. *European Journal of Protistology*, 40, 71–84. https://doi.org/10.1016/j.ejop.2003.11.002

52. Kundzewicz, Z. W., Mata, L. J., Arnell, N., Döll, P., Kabat, P., Jiménez, B., Miller, K., Oki, T., Şen, Z., & Shiklomanov, I. (2008). The implications of projected climate change for freshwater resources and their management. *Hydrological Sciences Journal*, 53, 3–10. https://doi.org/10.1623/hysj.53.1.3

53. Reynoldson, T. B. (1942). Vorticella as an indicator organism for activated sludge. *Nature*, 149, 608–609. https://doi.org/10.1038/149608b0

54. Madoni, P. (2011). Protozoa in wastewater treatment processes: A minireview. *Italian Journal of Zoology*, 78, 3–11. https://doi.org/10.1080/11250000903373797

55. Eisenmann, H., Letsiou, I., Feuchtinger, A., Beisker, W., Mannweiler, E., Hutzler, P., & Arnz, P. (2001). Interception of small particles by flocculent structures, sessile ciliates, and the basic layer of a wastewater biofilm. *Applied and Environmental Microbiology*, 67, 4286–4292. https://doi.org/10.1128/AEM.67.9.4286-4292.2001

56. Tchobanoglous, G., Stensel, D. H., Tsuchihashi, R., & Burton, F. (2014). *Wastewater engineering: Treatment and resource recovery* (5th ed.). McGraw-Hill Education.

57. Malul, D., Holzman, R., & Shavit, U. (2020). Coral tentacle elasticity promotes an out-of-phase motion that improves mass transfer. *Proceedings of the Royal Society B: Biological Sciences*, 287, 20200180. https://doi.org/10.1098/rspb.2020.0180

SUPPORTING INFORMATION

Additional supporting information can be found online in the Supporting Information section at the end of this article.

How to cite this article: Böttger, T., Klaassen van Oorschot, B., & Pepper, R. E. (2024). The effect of external flow on 3D orientation of a microscopic sessile suspension feeder, *Vorticella convallaria. Ann NY Acad Sci.*, *1537*, 51–63. https://doi.org/10.1111/nyas.15170